An angle-resolved dissociative photoionization study of the $c^4\Sigma^-_u$ state in O^+_2 using the TPEPICO technique

2010 J. Phys. B: At. Mol. Opt. Phys. 43 165204

(http://iopscience.iop.org/0953-4075/43/16/165204)

J. Phys. B: At. Mol. Opt. Phys. **43** (2010) 165204 (7pp) doi:10.1088/0953-4075/43/16/165204

An angle-resolved dissociative photoionization study of the $c^4\Sigma_u^-$ state in O_2^+ using the TPEPICO technique

A Padmanabhan[1], M A MacDonald[2], C H Ryan[2], L Zuin[2] and T J Reddish[1]

[1] Physics Department, University of Windsor, 401 Sunset Ave, Windsor, ON N9B 3P4, Canada
[2] Canadian Light Source, 101 Perimeter Road, Saskatoon, SK, S7N 0X4 Canada

E-mail: reddish@uwindsor.ca

Received 2 June 2010, in final form 7 July 2010
Published 30 July 2010
Online at stacks.iop.org/JPhysB/43/165204

Abstract

We have investigated the angular distributions of $O^+(^4S)$ ions produced from dissociative photoionization of O_2^+ $c^4\Sigma_u^-(v = 0, 1)$ using the TPEPICO technique, i.e. by measuring the coincidence yield between threshold photoelectrons and photoions. The vibrational levels have distinctly different lifetimes, τ_v, which diminish their inherent anisotropic photoion angular distribution characterized by a β parameter. We obtain $\tau_1 = 6.0 \pm 0.3 \times 10^{-14}$ s and a lower limit on τ_0 of $\approx 1 \times 10^{-12}$ s, in broad agreement with other experimental studies using different methods, and find that $\beta = 0.40 \pm 0.05$, which is significantly at variance with the predicted value of $\geqslant 1.6$.

1. Introduction

Inner valence photoionization of molecules can result in dissociative photoionization (DPI) into a variety of final states, and studies of both spectroscopy and fragmentation dynamics in this energy region continue to be theoretically and experimentally challenging, even for diatomic molecules. DPI is of great interest as, in the case of O_2 for example, it is a source of energetic ions and neutral species that contribute to the oxygen chemistry of the Earth's upper atmosphere [e.g. 1–3]. Moreover, O^+ ions, thought to be produced by DPI of O_2, have been recently observed in the tenuous atmosphere associated with Saturn's icy A ring system [4, 5]. This process together with dissociative ionization via charged particle collisions [6, 7] produces O^+ ions in other icy planetary regions, such as Jupiter's moons Europa and Ganymede [6–8]. Consequently, there is a sustained interest in processes that produce energetic oxygen ions and atoms.

In this work we restrict ourselves to the $c^4\Sigma_u^-$ state in O_2^+ at ~24.56 eV (above the O_2 $X^3\Sigma_g^-$ ground state), which has a shallow minimum in its potential well that supports two distinct quasi-bound vibrational levels ($v = 0$, 1). This existence of such a strongly predissociative state partly explains why there have been numerous theoretical and experimental studies of the $c^4\Sigma_u^-$ state over the years. As a dissociation product is metastable $O(^1D)$ atoms (only 1.97 eV above the ground state $O(^3P)$), this process also has direct relevance to stratospheric photochemistry [1–3].

DPI of O_2 between 20 and 28 eV has been recently explored in detail using electron–ion vector correlation methods, examining both the electron–ion kinetic energy correlation [9] and the molecular frame photoelectron angular distributions [10]. That latter study also gave laboratory frame ion angular distributions given by

$$\frac{d\sigma_{O^+}}{d\Omega} = \frac{\sigma_{O^+}}{4\pi}\left(1 + \beta_{O^+} P_2(\cos\theta)\right) = \frac{\sigma_{O^+}}{4\pi}\left(1 + \frac{\beta_{O^+}}{2}(3\cos^2\theta - 1)\right), \quad (1)$$

where θ is measured with respect to the polarization axis and is characterized by an asymmetry parameter, β_{O^+}, whose range lies between -1 and $+2$. In the case of the $c^4\Sigma_u^-$ state, the authors found a major discrepancy between their theoretical predictions and experimental observations. In [10] the authors determine β_{O^+} centred at ~1.9 eV (with $1.5 < E_{O^+} < 3.2$ eV) in coincidence with ~2.7 eV electrons (with $1.2 < E_e < 4.5$ eV) for a photon energy of 27.35 eV. Their measured β_{O^+} value was $\approx 0.1 \pm 0.05$. The effect of rotation, due to the lifetime, on

Table 1. The lowest five dissociative ionization channels in O_2^+ from [21, 22].

Label	Products	Dissociation energy (eV)
L1	$O(^3P) + O^+(^4S)$	18.733
L2	$O(^1D) + O^+(^4S)$	20.700
L3	$O(^3P) + O^+(^2D)$	22.057
L4	$O(^1S) + O^+(^4S)$	22.923
L5	$O(^3P) + O^+(^2P)$	23.750

the theoretical asymmetry parameter, $\beta^T_{O^+}$, for a non-rotating molecule is considered in [10] and found that β_{O^+} should reduce from ≈1.4 [11] to ≈0.8. That study also measured β_{O^+} to be ≈ 0 [3] and 0.35 for $\nu = 0$ and 1 levels, respectively, at ∼100 meV above their thresholds. Lafosse *et al* [10] recognized the appreciable discrepancy between theory and experiment and suggested that it could be due to either an underestimation in their apparatus function with large extraction fields or a lack of convergence in the calculation with respect to the inclusion of ions states. As this casts doubt on the reliability of the experimental study and, indeed, the technique, it is important to re-examine their findings using a different method.

The vibrational levels of the $c^4\Sigma_u^-$ state in O_2^+ have distinctly different lifetimes, τ_ν, due to predissociation, which reduces the state's inherent anisotropic photoion angular distribution for the non-rotating molecule. As will be reviewed below, there has been much discussion in the published literature on the τ_ν values, and the best experimental value (technically a 'lower limit') for τ_0 is ∼20 times smaller than current predictions. If one could have confidence in the theoretical asymmetry parameter for the $c^4\Sigma_u^-$ state, then an analysis of the observed ion angular distributions would give a direct measure of the lifetime as a function of the vibrational quantum number. Moreover, this approach would have general applicability to other predissociating states in diatomic molecules. The present experimental study therefore seeks to clarify the discrepancy observed by Lafosse *et al* [10] and provide further insight on the values of τ_ν. To place this work in context, we briefly outline current pertinent knowledge concerning the $c^4\Sigma_u^-$ state.

The $\nu = 1$ level dissociates almost exclusively to the $O(^1D) + O^+(^4S)$ dissociation limit (designated as L2—see table 1) at 20.700 eV [13–15]. The $\nu = 1$ level's decay to the L2 limit is due to tunnelling through the potential barrier and hence its lifetime, τ_1, is critically determined by the shape of the potential. Pulse-field ionization photoelectron (PFI-PE) experiments [16] determined τ_1 as $6.9 \pm 0.7 \times 10^{-14}$ s and this has been recently supported by theoretical studies [17, 18].

In contrast, the $\nu = 0$ level lives long enough to fluoresce to the $b^4\Sigma_g^-$ state [19, 20] and dissociative ionization competes with radiative decay. Two limits have been clearly established in the dissociative ionization channel, namely L1 and L2 (see table 1) with a branching ratio of approximately 1:2 [13, 14, 20, 21]. Akahori *et al* [14] also find a weak L5 contribution (∼5%) after subtracting L5 yield due to the underlying continuum, a background contribution that is also observed by [13, 15, 20]. Richard-Viard *et al* [20] conclude that decay to (a) the L2 limit occurs via tunnelling and (b) the L1 limit via the spin–orbit coupling to the $^4\Pi_u$ state. They also quantify the O^+/O_2^+ ratio as 6 ± 1 for the $\nu = 0$ level; i.e. an ∼15% fluorescence branching ratio.

An early theoretical study by Tanaka and Yoshimine [23] took the tunnelling lifetime for $\nu = 0$ to be the same as the estimated radiative lifetime, namely $\tau_f \sim 20 \times 10^{-9}$ s, resulting in equal probabilities of fluorescence and DPI for $\nu = 0$, i.e. $\tau_0 \sim 10 \times 10^{-9}$ s. However, using the fluorescence branching ratio, r, of ∼15% from [20] and

$$\frac{1}{\tau_0} \geqslant \frac{1}{r\tau_f} \tag{2}$$

reduces τ_0 to $\leqslant 3 \times 10^{-9}$ s. As is evident, reliable knowledge of the fluorescence lifetime would be extremely valuable, yet this does not appear to have been measured at this time. Tanaka and Yoshimine [23] also provide a number of theoretical calculations, one of which has τ values for $\nu = 0$, 1 two orders of magnitude smaller than their final values (see table 2). They considered those lifetimes to be too short, given the assumed value of τ_f.

The PFI-PE study of Evans *et al* [16], mentioned above, determined τ_0 to be $2.7 \pm 0.3 \times 10^{-13}$ s, four orders of magnitude smaller than that from [23]. Although the subsequent theoretical study by Liebel *et al* [24] generally favoured 'fast' dissociation over 'slow' dissociation of [23], the τ_0 value from [16] was criticized in the study by Hikosaka *et al* [18] as being too prompt. From their experimental data they place a lower limit on τ_0 as 6×10^{-13} s and introduce a qualitative theoretical model resulting in a τ_0 value of $\sim 1.3 \times 10^{-11}$ s, which they caution should be viewed as a 'very rough estimate'. Two further theoretical studies [17, 25] now report τ_0 to be $\approx 1.2 \times 10^{-11}$ s. Those studies, however, find ∼99% of the dissociative ionization results in L2; this agrees with experiment for $\nu = 1$, but not $\nu = 0$—as mentioned earlier, which has substantial decay to L1. These latter theoretical studies incorporated interactions between overlapping vibrational levels in the continuum, which reduces the slow dissociative ionization lifetimes from [23] by two orders of magnitude. The vibrational spacing of 0.192 eV corresponds to a vibrational period of 2.15×10^{-14} s. Using $\tau_0 = 1.2 \times 10^{-11}$ s and $\tau_1 = 6.9 \times 10^{-14}$ s implies that O_2^+ ($c^4\Sigma_u^-$) in the $\nu = 0$ and 1 levels execute ∼560 and 3 vibrations, respectively, prior to dissociation.

2. Experimental details

We have investigated the angular distributions of 2 eV $O^+(^4S)$ ions produced from DPI of O_2^+ $c^4\Sigma_u^-$ ($\nu = 0$, 1) using the threshold photoelectron–photoion coincidence (TPEPICO) technique. The experiments were performed using a dual toroidal spectrometer [26] in conjunction with linearly polarized synchrotron radiation on the VLS-PGM (undulator) beamline at the Canadian Light Source [27]. The apparatus has been previously used for (γ,2e) studies [e.g. 28] and threshold photoelectron spectroscopy (TPES) [29, 30];

[3] The earlier study of Eland and Duerr [12] using He(II) radiation also inferred β_{O^+} to be ≈0 for $\nu = 0$.

Table 2. Lifetimes of the vibrational levels of the O_2^+ $c^4\Sigma_u^-$ state.

$c^4\Sigma_u^-$	$v = 0$		$v = 1$		$v = 2$	
$h\upsilon$ (eV)	24.564[a]		24.756[a]		25.005[a]	
Theory/experiment	Γ_0 (meV)	τ_0 (s)	Γ_1 (meV)	τ_1 (s)	Γ_2 (meV)	τ_2 (s)
[23] T[b]	3.3×10^{-5}	20×10^{-9}	0.013	5×10^{-11}	1.6	4×10^{-13}
[23] T (SDCI)[b,c]	0.019	3.5×10^{-11}	3.6	1.8×10^{-13}		
[16] E	2.4	$2.7(3) \times 10^{-13}$	9.5	$6.9(7) \times 10^{-14}$		
[24] T[b]	0.19	3.4×10^{-12}	10.4	6.3×10^{-14}	167	3.9×10^{-15}
[18] E[d]	<1.1	$>6 \times 10^{-13}$	9.5	6.9×10^{-14}		
[18] T[d]	0.05	1.3×10^{-11}	9.5	6.9×10^{-14}		
[25] T[b]	0.056	1.17×10^{-11}	13.2	4.99×10^{-14}	112	5.88×10^{-15}
[17] T[b]	0.054	1.2×10^{-11}	9.7	6.8×10^{-14}	142	4.6×10^{-15}
This work	$< \approx 1$	$> \approx 1 \times 10^{-12}$	11.0 ± 0.5	$6.0 \pm 0.3 \times 10^{-14}$	120 ± 20	$\approx 5.5 \pm 1.0 \times 10^{-15}$

[a] From [35]. The calculated energies from [25] are 0.108 meV higher and the observed value for $v = 2$ in [15] is 24.96 eV.
[b] Predissociation lifetimes only, which are the dominant decay mechanism. However, when comparing with experimental values for the $v = 0$ level, one should note that the lifetime is slightly shorter (Γ_0 wider) than calculated due to the fluorescence channel.
[c] Single and double excitation configuration interaction (SDCI).
[d] 1.1 meV is their *upper* limit from experimental observation, corresponding to a *lower* limit on τ_0; 0.05 is an estimate from the model presented in [18]. They support [16] in their value for τ_1.

here we use the apparatus for ion–electron coincidences for the first time and so we briefly outline pertinent details.

The spectrometer consists of two toroidal analysers configured to detect charged particles emitted in the plane orthogonal to the incoming photon beam, which is crossed with an effusive gas jet emanating from a hypodermic needle as shown in figure 1. An adaptation of the penetrating-field technique [31] was used to extract efficiently and selectively near-zero energy electrons, which were then detected after passing through the smaller of the toroidal analysers. The details of the electron optical arrangement for TPES have been given in [29]. Two independent factors contribute to the overall energy resolution in TPES: (a) the photon beam resolution and (b) the threshold analyser response function. The former was estimated as 2.2 meV (FWHM) by fitting the rising edge of the He^+ ($n = 1$) TPES peak (see figure 3) to a Gaussian curve. The latter depends critically on (i) the strength of the extraction potential and (ii) the 'pass energy' of the energy analyser that is used to minimize the characteristic high-energy tail. The extraction potential needs to be high enough to remove the slowest electrons over 4π sr without being too high so that faster electrons are also pulled out over a large solid angle. There will always be some energetic electrons travelling in the direction of the extraction optics and these are eliminated by an energy dispersive device—in this case a toroidal analyser. The measured energy resolution in the threshold channel is 3.5 meV (FWHM) using He^+ ($n = 1$) at 24.586 eV (see figure 3).

The threshold electron extraction potentials have a tiny magnitude in the vicinity of the interaction region, such that all but the lowest of ion energies are transparent to the penetrating field. This allows one to perform angle-resolved coincidences between low-energy ions and threshold electrons. The ~2 eV $O^+(^4S)$ photoions emitted in the detection plane are energy analysed by the larger of the toroidal analysers with the acceptance angles and configuration indicated in figure 1. The focusing properties of the electrostatic analyser allow the charged particle's emission angle (measured relative to the light polarization axis) to be mapped onto a two-dimensional resistive anode encoder [26]. The energy-resolved image on the ion detector is arc-shaped with positions around the perimeter corresponding to the emission angle. A coincidence event is when both (ion and electron) detectors register a count within a specified time window, in this case 20 μs. In the TPEPICO data acquisition mode, $(x,y,\Delta t)$ are recorded for each coincidence event, where Δt is the time difference between the electron and the ion signal and (x,y) are the ion detection coordinates on the position-sensitive detector. Post-processing the Δt data as a time histogram shows a peak of 'true' coincidences upon a constant background of 'random' coincidences. The 'true' coincidence peak was ~1.5 μs wide (FWHM) and the true-random ratio was ~7:1. The corresponding ion (x,y) data are converted to the polar coordinates (r,θ) and the size of the angular intervals into which the data are processed is chosen later to correspond with

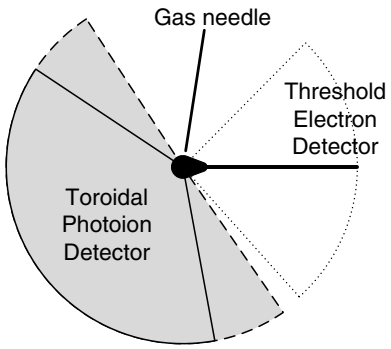

Figure 1. A schematic diagram of the acceptance angle ranges and the mutual configuration of the two toroidal analysers in our detection geometry. The photon beam is out of the page and the polarization direction is horizontal. The TPEPICO signal corresponds to the threshold electrons yield (over 4π sr) measured in coincidence with energy-resolved ions with emission angles within the central ~160° grey sector of the toroidal analyser, whose mechanical angular range is 180°. The out-of-plane emission angular acceptance in the ion channel is ~ ±10°.

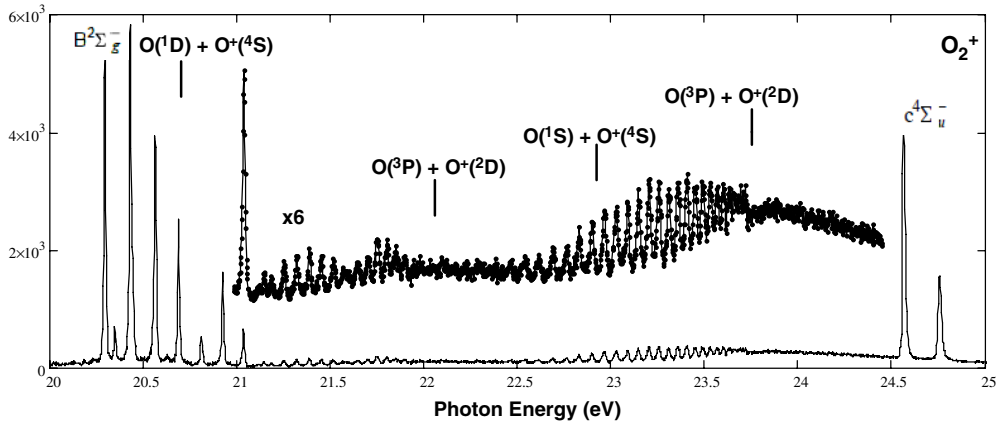

Figure 2. The threshold photoelectron spectrum for O_2^+ between 20 and 25 eV taken with an accumulation time of 4 s per point, in 2 meV steps, and a vacuum chamber pressure of $\sim 3 \times 10^{-6}$ torr. The dissociative ionization limits L2–5 are indicated (see table 1), as are the two most intense vibrational series: $B^2\Sigma_g^-$ and $c^4\Sigma_u^-$; the spectroscopy in this region discussed at length in [15, 33–37 and references therein].

the available statistics. In this case, 10° intervals in the angle θ_i were used for all the presented data. The 'true' coincidence angular distribution was obtained by subtracting the 'random' angular distribution from that of the total ('true' plus 'random') coincidence yield using standard procedures (see [26] and references therein). Since the random coincidence 'window' was 17.5 μs wide, seven times wider than the base width of the true 'window', this provided good statistical precision when subtracting these counts to obtain the true coincidences. The angular resolution, $\Delta\theta$, is deemed to be smaller than the angular interval based on our experience with (γ,2e) studies [28] and, when measuring the He^+ ($n = 1$) photoelectron angular distribution for 2 eV electrons, we observe the expected characteristic $\beta = 2$ pattern.

Due to axial recoil in a homonuclear diatomic molecule, the ion energy is simply given by

$$E_{O^+} = \tfrac{1}{2}(h\upsilon - D), \tag{3}$$

where the dissociation limit(s), D, is given in table 1. As the threshold photoelectron yield peaks at $h\upsilon = 24.564$ and 24.756 eV for $\nu = 0$ and 1 levels, respectively, the corresponding E_{O^+} values using equation (3) are 1.932 eV and 2.028 eV for the L2 dissociation limit. The toroidal analyser used to detect ions was operated with an energy resolution of $\approx\Delta E = 0.5$ eV, which is much broader than the ~100 meV spacing when set to detect 2.0 eV ions, and can readily separate ions from the neighbouring L1 and L3 limits.

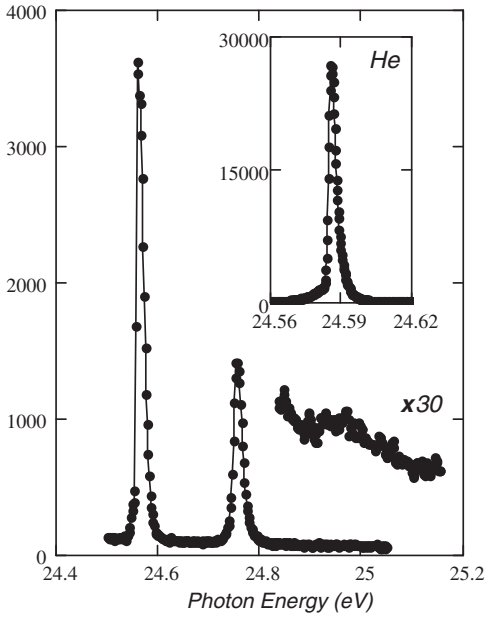

Figure 3. The threshold photoelectron spectrum for O_2^+ in the vicinity of the predissociative $c^4\Sigma_u^-$ state showing its three vibrational levels ($\nu = 0$–2) with progressively larger energy widths. As in figure 2, the accumulation time was 4 s per point, with 2 meV steps and a vacuum chamber pressure of $\sim 3 \times 10^{-6}$ torr. The inset shows the threshold photoelectron spectrum for He^+ ($n = 1$) in 0.25 meV steps used to determine the instrumental resolution, as discussed in the text.

3. Results and discussion

A survey threshold photoelectron spectrum displaying the states and dissociation limits between 20 and 25 eV is presented in figure 2. This O_2^+ spectrum is in excellent agreement with the earlier threshold studies of Guyon and Nenner [32], Ellis *et al* [15] and Tanaka *et al* [33]. That latter study had a resolution of ~2 meV FWHM in the 18–24 eV energy range and also used a supersonic beam to rotationally cool the molecules. The spectroscopy in this energy region has also been recently studied theoretically [34].

A zoomed region of the $c^4\Sigma_u^-$ state is shown in figure 3. As in other photoelectron studies [15, 31, 34], a very weak broad feature corresponding to $\nu = 2$ is observed at ≈24.97 eV on the sloping background of the $C^2\Sigma_u^-$ continuum [33]. We estimate its energy width to be ~120 ± 20 meV, which is larger than the 40 meV observed in [34] and in remarkable agreement with the predicted values given in table 2. We can also measure the increase in peak widths of the $\nu = 0$ and $\nu = 1$ vibration levels over the instrumental width determined earlier. The rotational profile [16, 25] shows that the main contribution to the *rising* edge of the threshold peak

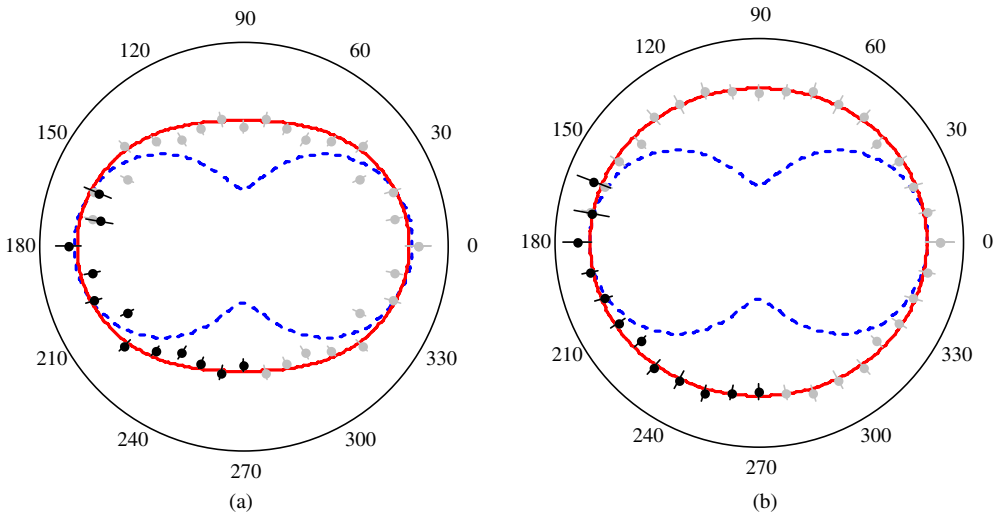

Figure 4. Polar plots of the *ratio* of the O^+ angular distributions to the L2 limit for the $v = 1{:}0$ levels of the $c^4\Sigma_u^-$ state measured in coincidence with a threshold photoelectron. The two graphs correspond to the ratio of (a) 'true' coincidences and (b) random coincidences (i.e. completely uncorrelated in time) at the two threshold photon energies, 24.756 and 24.564 eV. The measured black data points between 180° and 270° have been reflected in the x and y axes to give the grey points. The dashed curve corresponds to the ratio (arbitrarily normalized to the experimental data) using the following values of the asymmetry parameter and the lifetimes: $\beta^T_{O^+} = 1.6$, $\tau_0 = 1.2 \times 10^{-11}$ s and $\tau_1 = 6.0 \times 10^{-14}$ s. The solid curve is fitted to the measured data leading to $\beta^T_{O^+} = 0.40$; see the text for discussion.
(This figure is in colour only in the electronic version)

is from the 'P' branch, which is expected to extend over only a few meV depending upon rotational temperature. The procedure is to fit each peak to a Lorenzian lineshape over its rising edge from low photon energy to the peak maximum, which gives 4.2 ± 0.2 meV for $v = 0$ and 11.8 ± 0.4 meV for $v = 1$. As the rotational profiles of the $v = 0$ and $v = 1$ transitions are broadly similar [16] and since $\tau_0 \gg \tau_1$, we can use these values to estimate the increase in the $v = 1$ peak width due to lifetime broadening. Combining the values in quadrature gives a width of 11.0 ± 0.5 meV for $v = 1$ corresponding to a lifetime of $6.0 \pm 0.3 \times 10^{-14}$ s. This is in reasonable agreement with the only other measured value of $6.9 \pm 0.7 \times 10^{-14}$ [16] and the theoretical values given in table 2. Note that the lower limit on τ_1 from this study is $5.6 \pm 0.1 \times 10^{-14}$ s, based on the measured $v = 1$ peak width and the photon resolution.

In figure 4 we present the *ratio* of the O^+ angular distributions to the L2 limit for the $v = 1{:}0$ levels of the $c^4\Sigma_u^-$ state measured in coincidence with a threshold photoelectron. Unfortunately, we were not able to ascertain the individual ion angular distributions from these data due to (a) non-negligible systematic errors in the angular response of the toroidal analyzers and (b) the lack of a suitable calibrant of 2 eV ions with an accurately and reliably known β. However, the ratio of the angular distributions gives a relative measurement and has the advantage in that the systematic errors in the angular efficiency are effectively eliminated. Such ratios have been used previously to good effect [e.g. 38–40].

The ratio in figure 4(a) of the 'true' coincidence angular distribution corresponds explicitly to the $v = 1/v = 0$ yield:

$$\frac{\sigma^{v=1}_{O^+}\left(1 + \beta^{v=1}_{O^+} P_2(\cos\theta)\right)}{\sigma^{v=0}_{O^+}\left(1 + \beta^{v=0}_{O^+} P_2(\cos\theta)\right)}. \tag{4}$$

The ratio in figure 4(b) corresponds to the angular distribution of 2 eV O^+ ions at $h\upsilon = 24.756$ and 24.564 eV, namely

$$\frac{\left(\sigma^{v=1}_{O^+}\left(1+\beta^{v=1}_{O^+} P_2(\cos\theta)\right)+\sigma^{v=0}_{O^+}\left(1+\beta^{v=0}_{O^+} P_2(\cos\theta)\right)\right)_{24.756\text{eV}}}{\left(\sigma^{v=0}_{O^+}\left(1+\beta^{v=0}_{O^+} P_2(\cos\theta)\right)\right)_{24.564\text{eV}}}. \tag{5}$$

At 24.756 eV, 2eV O^+ ions can be produced by DPI from both $v = 1$ and 0 levels, unlike the lower photon energy which is below the $v = 1$ threshold. As mentioned above, the underlying continuum does not decay to L2, but to L5; hence, this does not contribute to the 2 eV ion yield. We take the relative proportion of $v = 1$ and 0 levels at the upper photon energy to be given by the ratio of the threshold photoelectron yield, namely 1:2.1, i.e. we make the approximation that the $v = 0$ cross section and $\beta^{v=0}_{O^+}$ at 24.756 eV to be the same as at 24.564 eV. Thus the measured angular distribution ratio in figure 4(b) is proportional to

$$\frac{\left(\sigma^{v=1}_{O^+}\left(\left(1+\beta^{v=1}_{O^+} P_2(\cos\theta)\right)+2.1\left(1+\beta^{v=0}_{O^+} P_2(\cos\theta)\right)\right)\right)_{24.756\text{eV}}}{\left(\sigma^{v=0}_{O^+}\left(1+\beta^{v=0}_{O^+} P_2(\cos\theta)\right)\right)_{24.564\text{eV}}}. \tag{6}$$

It is evident in figure 4(a) that the ratio distribution is slightly elongated along the polarization direction; from the form of (4) this implies $\beta_{v=1} > \beta_{v=0}$, which is primarily due to the differences in lifetimes.

To determine the ratios of (4) and (6), we may assume that the natural asymmetry parameter is independent of the vibrational quantum number. This allows us to use the expression given in [10] based on the earlier work of [12, 41], namely that the inherent or natural asymmetry parameter,

$\beta^T_{O^+}$ for a non-rotating molecule, which can only be obtained theoretically, is related to the observed or measured value via

$$\beta_{O^+} = \beta^T_{O^+}\left(\frac{1+a^2}{4+a^2}\right) \tag{7}$$

with $a = 1/(\omega\tau)$, where ω is the rotational velocity of the molecular state and τ is its lifetime. Note that when $\tau \to \infty$, $\beta_{O^+} \to \beta^T_{O^+}/4$ and as $\tau \to 0$, $\beta_{O^+} \to \beta^T_{O^+}$; thus, the effect of rotation is to reduce the inherent asymmetry parameter. We take the equilibrium internuclear separations for the $v = 0$ and 1 levels as 1.155 and 1.170×10^{-10} m respectively, from [16] and determine the average value for $\left(\frac{1+a^2}{4+a^2}\right)$ over a thermal distribution of rotational states, assuming that the gas emerging from the effusive gas source is at room temperature, for specific values of τ_0 and τ_1. The value of $\beta^T_{O^+}$ has, to our knowledge, only been determined by Lin and Lucchese [11]. They do not find a significant change in the $\beta^T_{O^+}$ values with the number of channels they include in their calculations and at threshold $\beta^T_{O^+} \geqslant 1.6$.

Using equations (4), (6) and (7) with $\beta^T_{O^+} = 1.6$, $\tau_0 = 1.2 \times 10^{-11}$ s from the published literature and $\tau_1 = 6.0 \times 10^{-14}$ s from this work we obtain a completely unacceptable ratio *shape* in comparison to the data (arbitrarily normalized), as shown in figure 4. We can find no agreement between the observed and theoretical ratio shape for any physically plausible values of τ_0 and τ_1. Hence, we conclude that there is something seriously amiss in the $\beta^T_{O^+}$ value suggesting that further work is needed in this regard.

Using $\tau_0 = 1.2 \times 10^{-11}$ s and $\tau_1 = 6.0 \times 10^{-14}$ s and keeping them constant results in $\beta^T_{O^+} = 0.38 \pm 0.07$ and 0.40 ± 0.05 for figures 4(a) and (b), respectively, giving essentially the same $\beta^T_{O^+}$ from the two different data sets and giving confidence to the approximations made in equation (6). The corresponding β_{O^+} values are 0.10 ± 0.02 and 0.30 ± 0.04 for $v = 0$ and 1 levels, respectively. These values are in good agreement with $\beta_{O^+} \approx 0$ and 0.35 observed in the earlier vector correlation study of Lafosse *et al* [10], indicating that the determination of their vector mapping apparatus function was reliable—despite their stated caution.

Although the results in the previous paragraph are obtained from using the 'best' values of τ_0 and τ_1 in equations (4), (6) and (7), we need to consider the effect of using other plausible values. Increasing τ_0 makes essentially no difference to the result, since β_{O^+} is close to its limit of $\beta^T_{O^+}/4$ for τ_0 (see equation (7)). If we take τ_0 as 6×10^{-13} s, the experimental lower limit from [18], we find $\beta^T_{O^+} = 0.40 \pm 0.07$ and 0.41 ± 0.06 for figures 4(a) and (b), respectively. If we take $\tau_1 = 6.9 \pm 0.7 \times 10^{-14}$ s, the consensus experimental and theoretical values from table 2 [16, 18], then we find $\beta^T_{O^+} = 0.42 \pm 0.07$. These values all cluster within error bars of the fit, so the uncertainties in the lifetimes τ_0 and τ_1 do not significantly affect the value of $\beta^T_{O^+}$.

4. Summary

In this TPEPICO study we use the high resolution of the threshold channel to define the vibrational level of the O_2^+ $c^4\Sigma_u^-$ state and examine the angular distribution of the ions, characterized by an angular asymmetry parameter, following DPI. Analysis of the observed asymmetry parameter allows one, in principle, to determine predissociation lifetimes and compare the results with those obtained by other experimental methods, such as deconvolution of the observed energy widths, and with theoretical predictions. To our knowledge, this method is rarely, if ever, used. Recent advances in ion momentum imaging techniques should make this more straightforward in future. We demonstrate that the judicious use of angular distribution *ratios* not only eliminates potential (and real) systematic errors in the observed angular distributions, but in special cases the need for a time-consuming coincidence experiment can be avoided altogether. Thus the technique we present here has a much wider application to other dissociative ionizing species. This study also highlights the need for accurate and reliable theoretical values of ion asymmetry parameters.

Our analysis of the ratio of the photoion angular distribution of $O^+(^4S)$ produced from DPI of O_2^+ $c^4\Sigma_u^-$ ($v = 0$, 1) also allows us to place a lower limit on τ_0 as $\approx 1 \times 10^{-12}$ s, corresponding to a width of $< \approx 1$ meV. This work, therefore, supports the experimental findings of [18]. There remains a factor ~20 difference between the experimentally determined lower limit of τ_0 and the current predicted values, even with this new experimental approach; narrowing that gap is a challenge for future work. The lack of sensitivity in being able to determine τ_0 more precisely, for a given τ_1, using this technique is partly due to the small value of the inherent asymmetry parameter $\beta^T_{O^+}$ for this particular ionic state. We have also determined τ_1 as $6.0 \pm 0.3 \times 10^{-14}$ s and $\beta^T_{O^+} = 0.40 \pm 0.05$, which is significantly smaller than predicted, $\beta^T_{O^+} \geqslant 1.6$, but in agreement with the experimental findings in [10]. Our estimate of the energy width of 120 ± 20 meV for the $v = 2$ level, corresponding to $\tau_2 = 5.5 \pm 1.0 \times 10^{-15}$ s, is in excellent agreement with the results of recent calculations [17, 24, 25].

Acknowledgments

The research described in this paper was performed at the Canadian Light Source, which is supported by NSERC, NRC, CIHR and the University of Saskatchewan. Furthermore, TJR and MAM acknowledge financial support from NSERC, the Universities of Windsor and Western Ontario and the Canadian Light Source. They also acknowledge Dr P Thorn (University of Western Australia) and Mr M Sullivan for their valuable contributions to this project.

References

[1] Rees M H 1989 *Physics and Chemistry of the Upper Atmosphere* (Cambridge: Cambridge University Press)
[2] Yung Y L and DeMore W B 1999 *Photochemistry of Planetary Atmospheres* (Oxford: Oxford University Press)
[3] Vardavas I M and Taylor F W 2007 *Radiation and Climate* (Oxford: Oxford University Press)
[4] Waite J H Jr *et al* 2005 *Science* **307** 1260–2
[5] Johnson R E *et al* 2006 *Icarus* **180** 393–402

[6] Luna H, McGrath C, Shah M B, Johnson R E, Liu M, Latimer C J and Montenegro E C 2005 *Astrophys. J.* **628** 1086–96
[7] Melo W S, Santos A C F, Sant'Anna M M, Sigaud G M and Montenegro E C 2008 *J. Phys. B: At. Mol. Opt. Phys.* **41** 205201
[8] Bagenal F, Dowling T E and McKinnon W B (eds) 2004 *Jupiter: The Planet, Satellites and Magnetosphere* (Cambridge: Cambridge University Press)
[9] Lafosse A, Brenot J C, Golovin A V, Guyon P M, Hoejrup K, Houver J C, Lebech M and Dowek D 2001 *J. Chem. Phys.* **114** 6605–17
[10] Lafosse A, Brenot J C, Guyon P M, Houver J C, Golovin A V, Lebech M, Dowek D, Lin P and Lucchese R R 2002 *J. Chem. Phys.* **117** 8368–84
[11] Lin P and Lucchese R R 2002 *J. Chem. Phys.* **116** 8863–75
[12] Eland J H D and Duerr E J 1998 *Chem. Phys.* **229** 1–11
[13] Frasinski L J, Randall K J and Codling K 1985 *J. Phys. B: At. Mol. Phys.* **18** L129–L135
[14] Akahori T, Morioka Y, Watanabe M, Hayaishi T, Ito K and Nakamura M 1985 *J. Phys. B: At. Mol. Phys.* **18** 2219–29
[15] Ellis K, Hall R I, Avaldi L, Dawber G, McConkey A, Andric L and King G C 1994 *J. Phys. B: At. Mol. Opt. Phys.* **27** 3415–26
[16] Evans M, Stimson S, Ng C Y and Hsu C W 1998 *J. Chem. Phys.* **109** 1285–92
[17] Demekhin F V, Omelýanenko D V, Lagutin B M, Sukhorukhov V L, Werner L, Ehresmann A, Schartner K-H and Schmoranzer H 2007 *Rus. J. Phys. Chem.* B **2** 213–21
[18] Hikosaka Y, Lablanquie P, Ahmad M, Hall R I, Lambourne, J G, Penent F and Eland J H D 2003 *J. Phys. B: At. Mol. Opt. Phys.* **36** 4311
[19] LeBlanc F J 1963 *J. Chem. Phys.* **38** 487–8
[20] Richard-Viard M, Dutuit O, Ait-Kaci M and Guyon P M 1987 *J. Phys. B: At. Mol. Phys.* **20** 2247–54
[21] Richard-Viard M, Dutuit O, Lavollee M, Govers T, Guyon P M and Durup J 1985 *J. Chem. Phys.* **82** 4054–63
[22] Hikosaka Y, Aoto T, Hall R I, Ito K, Hirayama R, Yamamoto N and Miyoshi E 2003 *J. Chem. Phys.* **119** 7693–700
[23] Tanaka K and Yoshimine M 1979 *J. Chem. Phys.* **70** 1626–33
[24] Liebel H, Ehresmann A, Schmoranzer H, Demekhin Ph V, Lagutin B M and Sukhorukov V L 2002 *J. Phys. B: At. Mol. Opt. Phys.* **35** 895–905
[25] Ehresmann A *et al* 2004 *J. Phys. B: At. Mol. Opt. Phys.* **37** 4405–22
[26] Reddish T J, Richmond G, Bagley G W, Wightman J P and Cvejanović S 1997 *Rev. Sci. Instrum.* **68** 2685–92
[27] Hu Y F *et al* 2007 *Rev. Sci. Instrum.* **78** 083109
[28] Wightman J P, Cvejanović S and Reddish T J 1998 *J. Phys. B: At. Mol. Opt. Phys.* **31** 1753–64
[29] Cvejanović S, Bagley G W and Reddish T J 1994 *J. Phys. B: At. Mol. Opt. Phys.* **27** 5661–79
[30] Slattery A E, Wightman J P, MacDonald M A, Cvejanović S and Reddish T J 2000 *J. Phys. B: At. Mol. Opt. Phys.* **33** 4833–48
[31] Cvejanović S and Read F H 1974 *J. Phys. B: At. Mol. Phys.* **7** 1180–92
[32] Guyon P M and Nenner I 1980 *App. Opt.* **19** 4068–79
[33] Tanaka T, Yoshii H, Morioka Y, Hayaishi T, Ito K and Hall R I 1998 *J. Chem. Phys.* **108** 6240–8
[34] Takeshita K, Sadamatu Y and Tanaka K 2005 *J. Chem. Phys.* **122** 044302
[35] Baltzer P, Wannberg B, Karlsson L, Göthe M C and Larsson M 1992 *Phys. Rev.* A **45** 4374–84
[36] Lu Y, He Z X, Cutler J N, Southworth S H, Stolte W C and Samson J A R 1998 *J. Electron Spectrosc.* **94** 135–47
[37] Shaw D A, Holland D M P, Rennie E E and Shpinkova L G 2005 *J. Phys. B: At. Mol. Opt. Phys.* **38** 173–88
[38] Reddish T J and Feagin J M 1999 *J. Phys. B: At. Mol. Opt. Phys.* **32** 2473–86
[39] Seccombe D P, Collins S A, Reddish T J, Selles P, Malegat L, Kazansky A L and Huetz A 2002 *J. Phys. B: At. Mol. Opt. Phys.* **35** 3767–80
[40] Kheifets A S and Bray I 2005 *Phys. Rev.* A **72** 022703
[41] Jonah C 1971 *J. Chem. Phys.* **55** 1915–22